

The applicability of isoconversional models in estimating the kinetic parameters of biomass pyrolysis

Érico de Godois Baroni¹  · Katia Tannous¹ · Yesid Javier Rueda-Ordóñez¹ · Lizeth Katherine Tinoco-Navarro¹

Received: 5 November 2014 / Accepted: 12 April 2015 / Published online: 13 May 2015
© Akadémiai Kiadó, Budapest, Hungary 2015

Abstract The objective of this study was to discuss the applicability of isoconversional models in estimating the activation energy and pre-exponential factor for biomass pyrolysis. Thermogravimetry and derivative thermogravimetry experiments of *tucumã* endocarp were performed at the heating rates of 5, 10, and 20 °C min⁻¹ in an atmosphere of nitrogen. The isoconversional models of Ozawa–Flynn–Wall, modified Coats–Redfern, Friedman, and Vyazovkin were applied to the experimental data, considering first-order rate law, resulting in activation energies of 147.25, 144.64, 160.47, and 144.96 kJ mol⁻¹, respectively. The pre-exponential factor varied from 9.75 to 11.95 log s⁻¹. As isoconversional models consider the solid decomposition to be represented by a single reaction, described by only one peak in the derivative thermogravimetry data, only a satisfactory agreement between experimental and theoretical data was observed. The fit was verified by simulating curves of conversion as a function of temperature, in which the kinetic parameters obtained with Ozawa–Flynn–Wall and Vyazovkin models generated the lowest relative deviations (9.05 and 9.3 %, respectively). In consequence, the use of isoconversional models is attractive because this kind of model is easy to apply, generating satisfactory approximations for the actual kinetic parameters.

Keywords *Astrocaryum aculeatum* · Activation energy · Pre-exponential factor · Reaction order

✉ Érico de Godois Baroni
ericobaroni@gmail.com

¹ School of Chemical Engineering, University of Campinas, Avenida Albert Einstein, 500, Cidade Universitária “Zeferino Vaz”, Campinas, SP 13083-852, Brazil

Introduction

Brazil is a developing country, and its economy is mostly agriculture based. Therefore, it is highly attractive that the widely available biomass materials, which include all residues generated by the agricultural and forestry activities, could be converted into a diversity of biofuels [1]. In the thermochemical route of conversion, pyrolysis represents a major step in which the complex kinetics is still unclear [2]. Pyrolysis is a thermochemical process that happens at temperatures of about 500 °C in an inert atmosphere (e.g., nitrogen), preventing combustion and gasification reactions to occur. In the thermal decomposition during pyrolysis, organic solids are converted into combustible liquids (tar), solids (biochar), and gases with a higher energy density than that of the feedstock [3]. At the present, lignocellulosic biomass is the main feedstock used in research papers about pyrolysis [4–6], especially because of its availability and renewable character [7].

In Brazil, the biofuels generated from biomass have been considered one of the solutions to overcome the lack of the electric power supply in isolated communities from the Amazonian region [1]. Various federal initiatives have been established in order to enable the utilization of lignocellulosic wastes as feedstock for, firstly, biofuel production through technologies such as pyrolysis, and secondly, conversion of these biofuels into electricity [8]. The first challenge in using biomass as a feedstock for pyrolysis is the inherent compositional variability of the different biomasses, what makes difficult to achieve a rather representative kinetic model that describes the thermal decomposition process [7].

The main goal of kinetic modeling is to estimate the kinetic parameters (E and A) that will represent the reaction contribution to the overall energy balance, providing ways

to optimize the reaction and to design industrial reactors [7, 9]. Traditionally, the modeling of pyrolysis kinetic is performed using semiempirical models that employ thermogravimetry (TG) and derivative thermogravimetry (DTG) results to estimate the kinetic parameters, considering the decomposition to occur in a single-step reaction. Among these, the isoconversional integral and differential models are equations widely used in pyrolysis kinetics, because they are able to estimate the activation energy requiring only a mathematical approximation for the temperature dependency [7]. However, when the pre-exponential factor and reaction order are to be estimated, it is mandatory to use an approximation for the composition dependency [10].

Integral and differential isoconversional models were developed in the 1960s mainly for the study of polymer decomposition [10, 11], being later extended to the study of biomass [9]. The adequacy of such models has long been debated not only because of their intrinsic mathematical limitations, but also due to the fact that different authors have presented discrepant results [7]. For example, [12] evaluated the kinetic parameters of hazelnut husk using three isoconversional integral models and obtained satisfactory results between conversions of 0.2 and 0.8, while the recommendation from the International Confederation for Thermal Analysis and Calorimetry (ICTAC) published by [9] clearly states that isoconversional models cannot describe the thermal decomposition behavior of complex materials such as biomass.

Therefore, the objective of this study is to discuss the applicability of the kinetic modeling of *tucumã* endocarp, an Amazon-native species, using four traditional isoconversional models, namely Ozawa–Flynn–Wall [10, 15], modified Coats–Redfern [11], Friedman [13], and Vyazovkin and Wight [24].

Theory

In isoconversional models, the reaction rate ($d\alpha \cdot dt^{-1}$) is defined as a product of a temperature-dependent and a conversion-dependent functions [11, 13]. According to [9], the temperature dependency is often approximated by the Arrhenius' law with accurate results. In addition, [7] states that usually an n th-order rate law is considered for the conversion dependency of biomass pyrolysis kinetics.

However, most published researches involving the kinetics of biomass pyrolysis using isoconversional models considered that the dependency on conversion (α) was represented by a simple first-order rate law, as in the researches developed by [12, 14], or the conversion dependency is not explicit and the pre-exponential factor (A) and reaction orders (n) are not given, as in the investigations of [4, 5].

For non-isothermal conditions, time and temperature can be exchanged in the reaction rate expression considering the

definition of heating rate, $\beta = dT \cdot dt^{-1}$. Hence, after variable separation and integration, Eq. (1) gives the reaction rate for non-isothermal conditions in terms of the Arrhenius' law (right-hand side) and the first-order rate law (left-hand side). In Eq. (1), E is the activation energy, R is the gas constant, and T is the absolute temperature.

$$-\ln(1 - \alpha) = g(\alpha) = \frac{A}{\beta} \int_{T_0}^T \exp\left(\frac{-E}{RT}\right) dT \quad (1)$$

The integral term in Eq. (1) does not have an analytical solution, and various methods were developed to estimate the kinetic parameters in this equation. Integral models arise from different numerical approximations for this integral [10, 11, 15], while differential models arise from a direct derivation that is free of approximations [13] but quite sensible to sudden changes in the reaction rate. For both integral and differential models, at least three sets of experimental data have to be used simultaneously in order to improve accuracy [9]. In addition, Eq. (2) can calculate the normalized mass (W) based on experimental data, in which m_0 is the initial sample mass and m_t is the sample mass at a given time.

$$W = 1 - \left(\frac{m_0 - m_t}{m_0}\right) \quad (2)$$

The experimental conversion was calculated using Eq. (3), in which the mass at the end of the experiments (m_f) was also taken into account.

$$\alpha = \left(\frac{m_0 - m_t}{m_0 - m_f}\right) \quad (3)$$

Materials and methods

Material

Astrocaryum aculeatum Meyer (*tucumã*) endocarp was the Amazonian biomass residue selected for this work since it can be used as a feedstock for locally producing biofuels through pyrolysis. *Tucumã* endocarp was obtained by [14] in *Aninga* community ($-2^{\circ}40'42.34''S \times -56^{\circ}46'32.35''W$), located in *Parintins* city, Amazon State, Brazil. The material was characterized, in which its physical, chemical, and thermal properties are shown in Table 1.

Reviewing the methodology applied by [14], the moisture content of the biomass was firstly quantified using the ASTM E871-82 [17] method. After that, the mean Sauter diameter of around 500 μm (by sieving) was selected because it was considered small enough to avoid the effects of heat and mass transfer between particles [16]. The

Table 1 Physical, chemical, and thermal properties of *tucumã* endocarp (adapted from [14])

Property	<i>Tucumã</i> endocarp
<i>Physical analyses</i>	
Mean Sauter diameter/ μm	499.41 ± 0.80
Apparent density/ kg m^{-3}	1115.01
True density/ kg m^{-3}	1442.60 ± 1.76
Sphericity/–	0.81 ± 0.04
Moisture/mass% wet basis	7.62 ± 0.05
<i>Elemental analysis/mass% dry basis</i>	
Carbon	47.99 ± 0.63
Hydrogen	5.99 ± 0.18
Nitrogen	0.29 ± 0.11
Sulfur	<0.1
Oxygen (by difference)	44.31
<i>Proximate analysis/mass% dry basis</i>	
Volatile matter	78.64 ± 0.20
Ash	1.45 ± 0.01
Fixed carbon	19.91 ± 0.21
<i>Heating value/MJ kg⁻¹</i>	
HHV	20.33 ± 0.34
LHV	17.27 ± 0.47

apparent density was determined by a mercury porosimeter, true density by a helium pycnometer, and particle sphericity by using the image processing software APO-GEO [18], version 1.0, considering Riley's equation (1941). The proximate analyses (volatile matter and ash contents in dry basis) were determined using the ASTM E872-82 [19] and ASTM E1755-01 [20] methods, respectively. The fixed carbon content was calculated by difference between these contents, completing 100 % of the mass. The ultimate analysis was quantified by using a CHNO elemental analyzer (Perkin Elmer, Series II 2400, USA), in which the oxygen content was calculated by difference with the carbon, hydrogen, and nitrogen contents. The sulfur content was determined by plasma atomic emission spectroscopy (Spectro, Arcos SOP, USA).

The higher heating value was determined using an adiabatic bomb calorimeter, applying the ASTM D240-09 [21] method, adapted by [22]. Additionally, the lower heating value was recalculated from [14] data using Mendeleev's equation (1949) [23], presented in Eq. (4), in which C, H, O, S, and U are the contents of carbon, hydrogen, oxygen, sulfur, and moisture, respectively.

$$\text{PCI} = 339\text{C} + 1030\text{H} - 109(\text{O} - \text{S}) - 25.2\text{U} \quad (4)$$

The samples presented a significant amount of volatile matter, what facilitates the decomposition process. In addition, the relatively low ash prevents operational

inconveniences, such as corrosion and fouling, which occur due to the presence of inorganics [3]. The samples also presented higher (HHV) and lower heating values (LHV) up to 20 MJ kg^{-1} .

Experimental setup

A thermogravimetric analyzer (Shimadzu Corp., TGA-50, Japan) was used by [14] to perform the thermal decomposition experiments with a measurement uncertainty of 0.001 mg. The samples were placed in an open sample platinum pan (6 mm internal diameter and 2.5 mm depth) with initial masses of $10.18 \pm 0.09 \text{ mg}$. The temperature was controlled from room temperature ($\sim 25 \text{ }^\circ\text{C}$) up to $900 \text{ }^\circ\text{C}$, at the heating rates of 5, 10, and $20 \text{ }^\circ\text{C min}^{-1}$. Data from three heating rates were used according to the recommendation of [9]. The remaining mass data were acquired with a time step of 5 s. High purity nitrogen (99.996 %) at a flow rate of 50 mL min^{-1} was used (4.6 FID from White Martins Inc., Campinas, Brazil). The equipment was purged with nitrogen 10 min before starting each run in order to avoid the sample oxidation. Both TG and DTG data were corrected by subtracting the experimental baselines for each heating rate.

Analysis and data processing

The thermogravimetry (TG) and derivative thermogravimetry (DTG) curves were analyzed using the TA-50WS software from Shimadzu Corporation (version 1.17). The mass data from TG/DTG were normalized by Eq. (2). The kinetic parameters, activation energy (E), and pre-exponential factor (A) were calculated using the program MS Excel 2013 (version 15.0.4641.1003).

Isoconversional kinetic models

In order to evaluate the kinetic parameters of the pyrolysis of *tucumã* endocarp, two integral isoconversional models were applied, namely Ozawa–Flynn–Wall [10, 15] and modified Coats–Redfern models [11], as well as the differential isoconversional model of Friedman [13]. Equations (5)–(7) give, respectively, the expressions for the Ozawa–Flynn–Wall (OFW), modified Coats–Redfern (MCR), and Friedman (FD) models, in which β is the heating rate, A is the pre-exponential factor, E is the activation energy, R is the ideal gas constant, T is the absolute temperature, and α is the conversion. The function $f(\alpha)$ in Eq. (7) is the differential form of the conversion-dependent function $g(\alpha)$, which was considered in this work to be represented by a first-order conversion function, left side of Eq. (1), in accordance with the works of [12] and [14].

$$\ln(\beta) = \ln\left(\frac{AE}{R}\right) - \ln[g(\alpha)] - 5.3305 + 1.052 \frac{E}{RT} \quad (5)$$

$$\ln\left[\frac{\beta}{T^2}\right] = \ln\left(\frac{AR}{E}\right) - \ln[g(\alpha)] - \frac{E}{RT} \quad (6)$$

$$\ln\left[\beta\left(\frac{d\alpha}{dT}\right)\right] = \ln[Af(\alpha)] - \frac{E}{RT} \quad (7)$$

The advanced model of Vyazovkin [24] was also applied using the corrected fourth degree Senum–Yang temperature integral approximation [25], $p(x)$, to calculate the kinetic parameters by minimizing an objective function (OF), given in Eq. (8). Equation (9) gives the temperature approximation derived by [25], in which x represents the reduced activation energy ($x = E R^{-1} T^{-1}$).

$$OF = \sum_{i=1}^N \sum_{j \neq i}^N \frac{J[E, T_i(t)]\beta_j}{J[E, T_j(t)]\beta_i} \quad (8)$$

$$J[E, T(t)] = \frac{E}{R} \cdot p(x) = \frac{\exp(-x)}{x} \cdot \frac{x^3 + 18x^2 + 86x + 96}{x^4 + 20x^3 + 120x^2 + 240x + 120} \quad (9)$$

The word isoconversional refers to the fact that this kind of kinetic model considers the activation energy to be a constant; consequently, it is necessary to perform the discretization of fixed values of conversion for which the calculation is made [26]. Therefore, in order to estimate the kinetic parameters, first it was necessary to calculate the experimental conversions using Eq. (3) and to discretize the values of conversion and temperature associated with them. In this step, normalized masses between 0.4 and 0.9 were selected (TG) to perform calculations, since this range represents the region with the highest volatilization content.

The series of calculations depicted in Fig. 1 were performed in order to apply the Ozawa–Flynn–Wall, modified Coats–Redfern, and Friedman models, in which steps a , b ,

and c relate to the calculation of the activation energy (E), while steps d and e relate to the optimization of the pre-exponential factor (A).

For Vyazovkin model (VZ), the activation energy was calculated using nonlinear regression to minimize Eq. (8), considering the combination of thermogravimetry data obtained at the three heating rates [24]. The pre-exponential factor was estimated simultaneously using Eq. (10). The conversion rate ($d\alpha \cdot dt^{-1}$), given in Eq. (11), was calculated using the TG (m_0 and m_f) and DTG ($dm \cdot dt^{-1}$) results.

$$A = \frac{d\alpha}{dt} \left(\frac{1}{1-\alpha}\right) \left[\frac{1}{\exp(-E/RT)}\right] \quad (10)$$

$$\frac{d\alpha}{dt} = \left(\frac{-dm}{dt}\right) \cdot \left(\frac{1}{m_0 - m_f}\right) \quad (11)$$

Verification of kinetic parameters

The verification of the kinetic parameters obtained by applying OFW, MCR, FD, and VZ models was performed by simulating curves of conversion as a function of temperature. The average values for E and A were used to calculate the theoretical conversion rate ($\alpha_{i,sim}$), given in Eq. (12). Conversions were numerically calculated by using Euler’s explicit method, considering an integration step of 5 s, as means to maintain consistency with experimental measurements. A first-order conversion function was also considered in the simulations. Equation (13) presents the total sum of squares (SS) between experimental ($\alpha_{i,exp}$) and simulated conversions ($\alpha_{i,sim}$), used to calculate the relative deviations, given in Eq. (14), in which N is the total number of experimental measurements used in the simulations [27]. The numbers of experimental measurements were equal to 596, 299, and 150 points for the heating rates of 5, 10, and 20 °C min⁻¹, respectively.

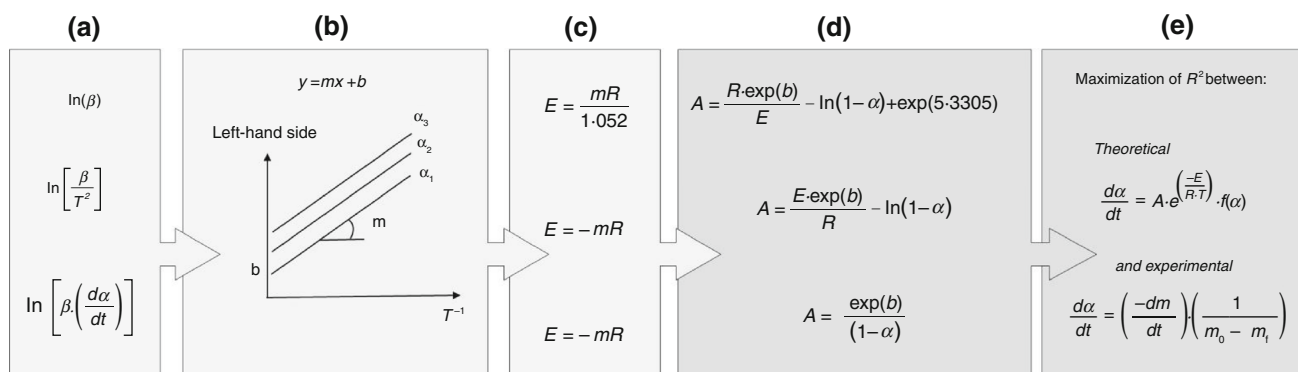


Fig. 1 Flowchart for calculating the activation energy and pre-exponential factor using isoconversional models (OFW, MRC, and FD). **a** Calculation of the left-hand side, **b** linearization for each level of α , **c** calculation of E , **d** first estimation of A ($n = 1$), **e** optimization of A and E

$$\frac{d\alpha}{dt} = A \exp\left(\frac{-E}{RT}\right) (1 - \alpha) \quad (12)$$

$$SS = \sum_{i=1}^N (\alpha_{i,\text{exp}} - \alpha_{i,\text{sim}})^2 \quad (13)$$

$$\text{Relative deviation} = 100 \sqrt{\frac{SS}{N}} \quad (14)$$

Results and discussion

Thermal analysis

Thermogravimetry (TG) and derivative thermogravimetry (DTG) curves obtained by [14] were used to investigate the thermal behavior and the kinetics of *tucumã* endocarp in an inert atmosphere at three heating rates. Figure 2a shows the TG curve in terms of the normalized mass, calculated according to Eq. (2), while Fig. 2b presents the DTG of the *tucumã* endocarp.

Observing the normalized mass curve, the thermal decomposition was divided into three main events. The first one is between room temperature and approximately 150 °C, the second is between 150 and 450 °C, and the last one is between 450 and 900 °C. The percentage variations

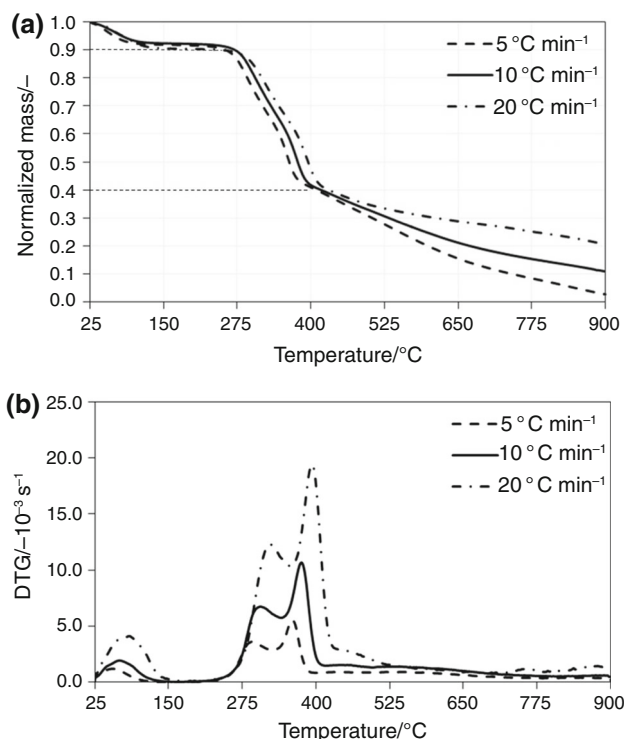


Fig. 2 Thermogravimetry (a) and derivative thermogravimetry (b) curves of the *tucumã* endocarp (adapted from [14])

associated with these three decomposition events are given in Table 2 for the three heating rates.

The first decomposition event was related to the release of water and extractives [28], and it can also be observed as the first peak in the DTG curve. In the second event, the highest decreases in the normalized mass were observed. Therefore, they were associated with the decomposition of hemicellulose and cellulose (second and third peaks in the DTG) as well as part of lignin [29]. However, as lignin presents a wider range of thermal stability, i.e., it continues to decompose at temperatures higher than 500 °C [28], the third decomposition event was attributed to the decomposition of these more stable intermediary compounds of lignin and also recombining reactions among the gaseous, liquid, and solid products [30].

Application of isoconversional models

The kinetic modeling using the isoconversional equations proposed by Ozawa–Flynn–Wall (OFW), modified Coats–Redfern (MCR), Friedman (FD), and Vyazovkin (VZ) was performed in order to estimate the activation energy (E) and pre-exponential factor (A), using non-isothermal thermogravimetry experiments obtained at 5, 10, and 20 °C min⁻¹.

Initially, the experimental conversions were calculated using Eq. (3), and levels between 0.10 and 0.90 were discretized, in order to perform isoconversional calculations. For OFW, MCR, and FD models, the series of calculations depicted in Fig. 1 was followed and the optimized kinetic parameters were obtained. The linearization plots, step b) in Fig. 1, are shown in Fig. 3 for the OFW, MCR, and FD models. For VZ model, the activation energy was estimated using Eqs. (8) and (9), while the pre-exponential factor was calculated by using Eqs. (10) and (11).

The linearization plots for both integral models are marked by a parallelism among the linear regressions obtained at each conversion level, as it was expected from isoconversional models. However, in the linearization for the differential model of Friedman, for conversion higher than 0.50, the regression curves present a change in the parallelism (dashed lines), what could be an indicative of the occurrence of multiple reactions. This behavior is not observed in the integral models because they are not

Table 2 Main decomposition events observed in the TG and DTG curves of the *tucumã* endocarp (adapted from [14])

Heating rate/°C min ⁻¹	1st event/mass%	2nd event/mass%	3rd event/mass%
5	8.12	56.11	32.87
10	8.68	55.28	26.00
20	9.45	52.45	17.31

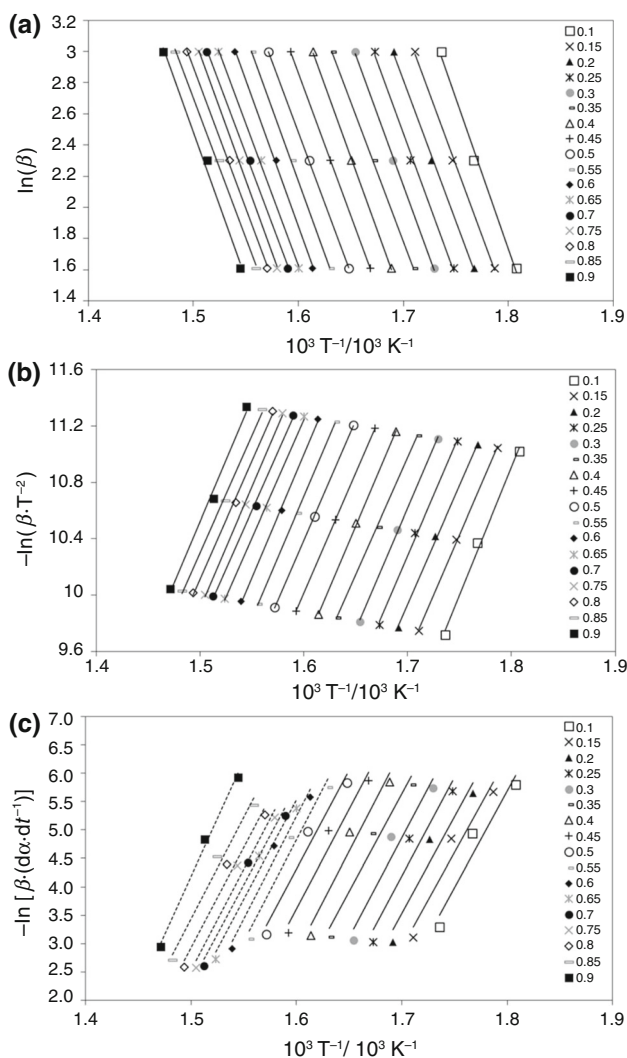


Fig. 3 Linearization plots for the isoconversional models of OFW (a), MCR (b), and FD (c)

directly based on the reaction rate data, being less sensible to concavity changes in the curve of the reaction rate as a function of conversion. Nevertheless, for all isoconversional models and conversion levels, determination coefficients (R^2) higher than 0.99 were obtained.

As means to compare the results obtained with isoconversional models, Fig. 4 presents the distribution of activation energy with conversion. Table 3 summarizes the average optimized kinetic parameters calculated between conversions of 0.10 and 0.90.

Three conversion intervals are shown in Fig. 4, representing predominantly the decomposition of hemicellulose ($0.15 \leq \alpha \leq 0.30$), hemicellulose + cellulose ($0.40 \leq \alpha \leq 0.60$), and cellulose ($0.60 \leq \alpha \leq 0.85$), respectively. The wavering of the activation energy with the conversion is related with the shifts in the concavity of the reaction rate curve (Fig. 2b), reaching minimum at $\alpha = 0.35$, $\alpha = 0.7$,

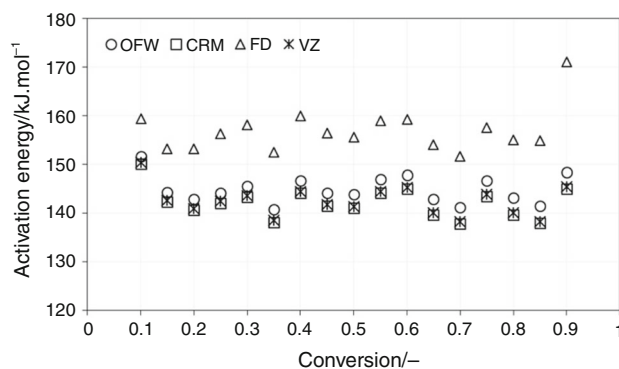


Fig. 4 Activation energy as a function of conversion for the OFW, MCR, FD, and VZ models

Table 3 Averages and standard deviations of E and A calculated with isoconversional models

Model	$E/\text{kJ mol}^{-1}$	$\log(A)/\log \text{s}^{-1}$
Ozawa–Flynn–Wall [10, 15]	147.25 ± 7.81	9.91 ± 1.04
Modified Coats–Redfern [11]	144.64 ± 8.22	11.95 ± 1.11
Friedman [13]	160.47 ± 13.44	11.65 ± 1.10
Vyazovkin and Wight [24]	144.96 ± 8.24	9.75 ± 0.83

and $\alpha = 0.85$. The extremal conversion levels, 0.1 and 0.9, represent the final stage of moisture release and the beginning of the decomposition of majorly lignin, respectively. Thus, each one of these peaks could be interpreted as an independent reaction.

The kinetic parameters (Table 3) calculated were in a similar magnitude, in which the activation energy presented the highest standard deviation among models. The MCR model resulted in the lowest standard deviation, followed by the VZ, OFW, and FD models. The application of MCR and VZ models generated practically identical values for E (144 kJ mol^{-1}). The OFW model presented a difference of about 4 kJ mol^{-1} , while the difference for the FD model was approximately 16 kJ mol^{-1} . [12] also observed that the activation energy estimated with MCR models is lower than the one for OFW, being a characteristic of models that come from different approximations for the temperature integral used to solve Eq. (1). In addition, the estimates for the pre-exponential factor are in a physically acceptable magnitude and, as the activation energy, they should be close to the actual kinetic parameters.

In order to compare the activation energies calculated in this work ($E_{\text{our_work}}$), Table 4 presents the experimental conditions, average activation energy ($E_{\text{literature}}$), percentage difference, and kinetic models applied by some recent studies regarding biomass pyrolysis.

The activation energies calculated in this work ($144\text{--}160 \text{ kJ mol}^{-1}$) are close to the ones reported by the literature and exposed in Table 4. Comparing the

Table 4 Comparison of the apparent activation energy calculated for *tucumã* endocarp with some biomass from literature

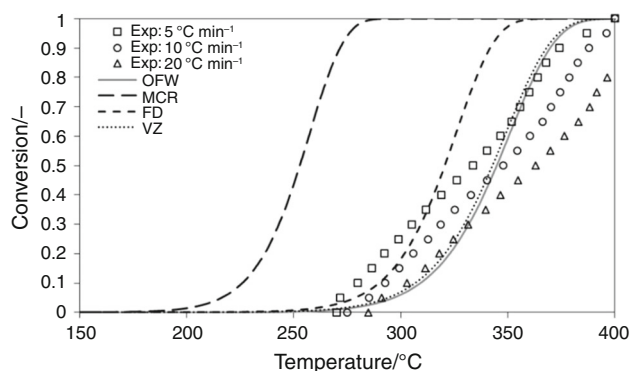
Biomass	Experimental Gas flow/mL min ⁻¹ $\beta/^\circ\text{C min}^{-1}$ $\bar{d}_p/\mu\text{m}$	Model	$E/\text{kJ mol}^{-1}$	Percentage difference ^a /%	Reference
<i>Tucumã</i> endocarp	Gas flow: 50 (N ₂) β : 5, 10, 20 \bar{d}_p : 499.41	OFW	147.25 ± 7.81	–	This work
		MCR	144.64 ± 8.22		
		FD	160.47 ± 13.44		
		VZ	144.96 ± 8.24		
<i>Tucumã</i> endocarp	Gas flow: 50 (N ₂) β : 5, 10, 20, 40 \bar{d}_p : 499.41	OFW	134.43 ± 4.31	8.71	[14]
Hazelnut husk	Gas flow: 80 (N ₂) β : 5, 10, 20 \bar{d}_p : 63–125	OFW	131.10 ± 21.26	10.97	[12]
		MCR	127.82 ± 23.35	11.63	
Cacao shells	Gas flow: 80 (N ₂) β : 5, 10, 15, 20 \bar{d}_p : 63–125	OFW	145.6	1.12	[31]
		FD	127.7	20.42	
Rice straw	Gas flow: 100 (N ₂) β : 5, 10, 20, 30, 40 \bar{d}_p : 50	OFW	146.64 ± 66.05	0.41	[32]
		MCR	178.42 ± 50.47	–23.35	
		FD	195.17 ± 58.81	–21.62	
		VZ	168.58 ± 61.18	–16.29	

$$^a \text{Percentage difference} = 100 \left(\frac{E_{\text{our_work}} - E_{\text{literature}}}{E_{\text{our_work}}} \right)$$

activation energy calculated in this work ($E_{\text{our_work}}$) with the activation energy estimated by the literature ($E_{\text{literature}}$), [14] obtained activation energies 8.71 % lower, using OFW model for *tucumã* endocarp pyrolysis. This difference is probably related to that fact that [14] used thermogravimetry data obtained at $\beta \geq 20^\circ\text{C min}^{-1}$. For the other models shown in Table 4, the maximum percentage differences were calculated: 10.97 % (OFW—hazelnut husk); –23.35 % (MCR—rice straw); 20.42 % (FD—rice straw), and –16.29 % (VZ—rice straw). No work was found in the literature regarding the application of MCR, FD, and VZ models to *tucumã* endocarp. Therefore, these differences were little representative, considering the composition variation in the different biomasses. The standard deviations (Table 4) indicate that the activation energies calculated in this work are in agreement with the ones reported in the literature, what shows the consistency of the activation energies here calculated.

Verification of isoconversional kinetic parameters

Simulations performed the verification of adequacy of the activation energies (E) and pre-exponential factors (A) calculated using Ozawa–Flynn–Wall, modified Coats–Redfern, Friedman, and Vyazovkin models in describing the thermal decomposition process, as shown in Fig. 5. The average E and A presented in Table 3 were used to simulate

**Fig. 5** Comparison between experimental and theoretical (OFW, MCR, FD, and VZ models) conversions as a function of temperature

curves of conversion as a function of temperature for each isoconversional model. The theoretical conversion rate given in Eq. (12) was numerically integrated from 150 to 400 °C, in order to account only the region of the highest volatilization. Figure 5 shows the simulations together with the experimental conversions ($\beta = 5, 10, \text{ and } 20^\circ\text{C min}^{-1}$), calculated using Eq. (3).

The simulations for OFW, FD, and VZ models presented a good agreement with the experimental conversions calculated at all heating rates. However, the curve simulated with the average kinetic parameters estimated with MCR model deviated considerably from the

Table 5 Relative deviations between experimental and simulated conversion curves

Models	Heating rate/°C min ⁻¹		
	5	10	20
Ozawa–Flynn–Wall [10, 15]	18.25	12.95	9.05
Modified Coats–Redfern [11]	50.60	51.75	53.50
Friedman [13]	21.27	24.04	27.83
Vyazovkin and Wight [24]	18.80	13.42	9.30

experiments, with a temperature displacement of about 80 °C. This difference is due to the elevated pre-exponential factor calculated with the MCR model, comparatively to VZ model, since both present practically the same average activation energy. The simulation for FD model also presented a displacement (~40 °C), while OFW and VZ simulations were the closest to the experimental results. In order to evaluate the fit between experimental and simulated conversion values, the relative deviations were calculated for all isoconversional models, according to Eqs. (13) and (14). The relative deviations for each heating rate are presented in Table 5.

Due to the temperature displacement observed in Fig. 5, the curves simulated using the average kinetic parameters of MCR and FD models presented an increase in the relative deviation with increasing heating rates. As exposed in Table 4, [12] also applied MCR model, verifying qualitatively a displacement of the theoretical curves toward lower temperatures and considerable deviations from the experimental behavior. Additionally, the lowest relative deviations were obtained applying OFW and VZ kinetic parameters. The results for both models were very similar, in which lower relative deviations (~9 %) were calculated for the faster heating rate (20 °C min⁻¹). Therefore, the application of the isoconversional models generated satisfactory agreement with the experimental behavior, since *tucumã* endocarp presents a complex decomposition profile (Fig. 2b).

Nevertheless, the easy mathematical application of such models is attractive especially when compared with more tangled models such as the ones that consider independent parallel reactions for the main components of biomass [4, 5]. Due to intrinsic limitations of the models and to the compositional variability of biomass, this kind of model fits more adequately biomasses that present just one peak in their DTG. However, when used for biomass that presents more than one peak in the DTG, such as *tucumã* endocarp, the kinetic parameters obtained using isoconversional models can only be considered approximations of the actual values, generating kinetic parameters that represent satisfactorily the decomposition profile of biomass.

Conclusions

Isoconversional models are an initial step to the modeling of thermal decomposition, because they are easily applied. However, the kinetic parameters calculated using this kind of model represent the actual kinetic parameters only for biomass that presents or resembles simply one peak in the DTG. Nevertheless, the simulations showed that the kinetic parameters calculated with Ozawa–Flynn–Wall and Vyazovkin models presented a rather satisfactory agreement with experimental data, considering the very complex decomposition profile of *tucumã* endocarp. In the next step of this work, aiming an improved fit, reaction schemes that consider the decomposition to occur by independent parallel reactions will be applied, taking into account the contribution of the mass fractions of each main component of biomass.

Acknowledgements The authors are thankful for the financial support received from the Coordination for the Improvement of Higher Education Personnel (CAPES), Brazil.

References

- Lora ES, Andrade RV. Biomass as energy source in Brazil. *Renew Sustain Energy Rev.* 2009;13:777–88.
- Van de Velden M, Baeyens J, Brems A, Janssens B, Dewil R. Fundamentals, kinetics and endothermicity of the biomass pyrolysis reaction. *Renew Energy.* 2010;35:232–42.
- Basu P. Biomass gasification and pyrolysis—practical design. Oxford: Academic Press; 2010. p. 23–92.
- Anca-Couce A, Berger A, Zobel N. How to determine consistent biomass pyrolysis kinetics in a parallel reaction scheme. *Fuel.* 2014;123:230–40.
- Cardoso CR, Miranda MR, Santos KG, Ataíde CH. Determination of kinetic parameters and analytical pyrolysis of tobacco waste and sorghum bagasse. *J Anal Appl Pyrolysis.* 2011;92:392–400.
- Mohan D, Pittman CU, Steele PH. Pyrolysis of wood/biomass for bio-oil: a critical review. *Energy Fuels.* 2006;20:848–89.
- White JE, Catallo WJ, Legendre BL. Biomass pyrolysis kinetics: a comparative critical review with relevant agricultural residue case studies. *J Anal Appl Pyrolysis.* 2011;91:1–33.
- Gómez MF, Silveira S. Rural electrification of the Brazilian Amazon—achievements and lessons. *Energy Policy.* 2010;38:6251–60.
- Vyazovkin S, Burnham AK, Criado JM, Pérez-Maqueda LA, Popescu C, Sbirrazzuoli N. ICTAC Kinetics Committee recommendations for performing kinetic computations on thermal analysis data. *Thermochim Acta.* 2011;520:1–19.
- Flynn JH, Wall LA. General treatment of the thermogravimetry of polymers. *J Res Natl Bur Stand.* 1934;1966(70):487–523.
- Braun RL, Burnham AK, Reynolds JG, Clarkson JE. Pyrolysis kinetics for lacustrine and marine source rocks by programmed micro-pyrolysis. *Energy Fuels.* 1991;5:192–204.
- Ceylan S, Topçu Y. Pyrolysis kinetics of hazelnut husk using thermogravimetric analysis. *Bioresour Technol.* 2014;156C:182–8.
- Friedman HL. Kinetics of thermal degradation of char-forming plastics from thermogravimetry. Application to a phenolic plastic. *J Polym Sci Part C Polym Symp.* 1964;6:183–95.

14. Nascimento VF. Caracterização de biomassas amazônicas—ouríço de castanha-do-brasil, ouríço de sapucaia e caroço do fruto do tucumã—visando sua utilização em processos de termoconversão. Master's Dissertation, University of Campinas. 2012, p. 148.
15. Ozawa T. A new method of analyzing thermogravimetric data. *Bull Chem Soc Jpn.* 1965;707:1881–6.
16. Cai J, Wu W, Liu R, Huber GW. A distributed activation energy model for the pyrolysis of lignocellulosic biomass. *Green Chem.* 2013;15:1331.
17. ASTM—American Society for Testing and Materials Standard D240. Standard test method for heat of combustion of liquid hydrocarbon fuels by bomb calorimeter. West Conshohocken: ASTM International; 2009. doi:[10.1520/D0240-09](https://doi.org/10.1520/D0240-09).
18. Tannous K, Silva FS. Particles and geometric shapes analyzer APOGEO. In: Khosrow-Pour M, editor. *Encyclopedia of information science and technology*. 3rd ed. doi:[10.4018/978-1-4666-5888-2.ch349](https://doi.org/10.4018/978-1-4666-5888-2.ch349).
19. ASTM Standard Standard E1755, 2001. Standard test method for ash in biomass. West Conshohocken: ASTM International; 2007. doi:[10.1520/E1755-01R07](https://doi.org/10.1520/E1755-01R07).
20. ASTM Standard E871, 1982. Standard test method for moisture analysis of particulate wood fuels. West Conshohocken: ASTM International; 2006. doi:[10.1520/E0871-82R06](https://doi.org/10.1520/E0871-82R06).
21. ASTM Standard E872, 1982. Standard test method for volatile matter in the analysis of particulate wood fuels. West Conshohocken: ASTM International; 2006. doi:[10.1520/E0872-82R06](https://doi.org/10.1520/E0872-82R06).
22. Sánchez C. Caracterização das biomassas. In: SÁNCHEZ C (Org.). *Tecnologia da gaseificação de biomassa*. Campinas, Sao Paulo, Brazil: Editora Átomo, pp. 200–209, 2010.
23. Mendeleev DI. Compositions (collection of works). Reports from the Science Academy of Union of Soviet Socialist Republics: Moscow, vol. 15, p. 115–118, 1949.
24. Vyazovkin S, Wight CA. Isothermal and nonisothermal reaction kinetics in solids: in search of ways toward consensus. *J Phys Chem.* 1997;5639:8279–84.
25. Senum GI, Yang RT. Rational approximations of the integral of Arrhenius function. *J Therm Anal.* 1977;11:445–7.
26. Coats AW, Redfern JP. Kinetic parameters from thermogravimetric data II. *J Polym Sci Part B Polym Lett.* 1965;3:917–20.
27. Órfão JJM, Antunes FJA, Figueiredo JL. Pyrolysis kinetics of lignocellulosic materials—three independent reactions model. *Fuel.* 1999;78:349–58.
28. Raveendran K, Ganesh A, Khilar KC. Pyrolysis characteristics of biomass and biomass components. *Fuel.* 1996;75:987–98.
29. Di Blasi C. Modeling chemical and physical processes of wood and biomass pyrolysis. *Prog Energy Combust Sci.* 2008;34:47–90.
30. Shen J, Wang XS, Garcia-Perez M, Mourant D, Rhodes MJ, Li CZ. Effects of particle size on the fast pyrolysis of oil mallee woody biomass. *Fuel.* 2009;88:1810–7.
31. Biagini E, Fantei A, Tognotti L. Effect of the heating rate on the devolatilization of biomass residues. *Thermochim Acta.* 2008;472:55–63.
32. Mishra G, Bhaskar T. Non isothermal model free kinetics for pyrolysis of rice straw. *Bioresour Technol.* 2014;169:614–21.